

Polyvinyl Alcohol (PVA)-assisted Synthesis of BiFeO₃ Nanoparticles for Photocatalytic Applications

Feng Niu, Tong Gao, Laishun Qin, Zhi Chen, Qiaoli Huang, Ning Zhang,
Sen Wang, Xingguo Sun and Yuexiang Huang*

College of Materials Science and Engineering, China Jiliang University, Hangzhou 310018, Zhejiang, P.R. China

Received: January 13, 2015, Accepted: March 20, 2015, Available online: June 30, 2015

Abstract: Bismuth ferrite (BiFeO₃) is a promising material for visible light response photocatalytic applications. In the present work, BiFeO₃ particles were synthesized by a polyvinyl alcohol (PVA)-assisted solid state reaction processing. The XRD pattern result indicated that the as-prepared particles are pure BiFeO₃ crystalline phase. The microscopy observation demonstrated that the BiFeO₃ particle size is from 100 to 200 nm, which is smaller than that of the BiFeO₃ prepared without addition of PVA. The HRTEM showed that BiFeO₃ particle is polycrystalline and contains many small crystal grains with different orientations. Furthermore, such nanosized and well-dispersed BiFeO₃ particles exhibited a much higher photocatalytic activity than the prepared BiFeO₃ without addition of PVA for the photodegradation of methyl orange contaminant under visible light irradiation.

Keywords: bismuth ferrite; polyvinyl alcohol; solid state synthesis; microstructure; photoelectrochemistry;

1. INTRODUCTION

Bismuth ferrite (BiFeO₃, noted as BFO) is one of the most investigated single-phase multiferroic materials because of its coexistence of ferroelectric and antiferromagnetic orders with ferroelectric Curie temperature $T_C = 830$ °C and an antiferromagnetic Neel temperature $T_N = 370$ °C, which allows it to be a promising material for the application in multiferroic memories [1]. In addition to magnetoelectric applications, BFO can also be considered as a potential photocatalyst due to its small band gap (~2.5 eV), chemical stability and easy availability [2]. Comparing with the widely-used TiO₂ photocatalyst (~3.2 eV [3]), the small band gap of BFO material allows the effort of extending the photocatalytic response to visible light region to become possible. In a previous report [4], it has been revealed that BFO particles demonstrate a capability of degrading the methyl orange (MO) under the visible light irradiation. However the photocatalytic activity is largely dependent on the particle morphology, size, phase purity, dispersity and crystallinity of the obtained BFO material [5]. Therefore developing a controllable and low cost processing method to synthesize BFO particles with characteristics of nanosized, pure crystalline phase with well dispersity is still a big challenge for both

scientists and engineers.

Currently most BFO particles are synthesized by solid state reaction or wet chemical methods including co-precipitation, hydrothermal, sol-gel, microemulsion technique, etc. [6-12]. Among them the solid state reaction processing method is particularly interesting because it could produce BFO particles on an industrial scale at a relatively low cost. In a typical solid state reaction route, bismuth hydroxide and ferric hydroxide are co-precipitated by potassium hydroxide from a ferric nitrate and bismuth nitrate solution. After washing and drying, the precipitate is calcined at a temperature ranging from 500 °C to 900 °C to get BFO powders [13]. Such a processing route, however, would generally lead to the presence of secondary crystalline phases such as Bi₂O₃, Bi₂Fe₄O₉ and Bi₂₅FeO₄₀ and heavily particle agglomerations are generally observed [4], which would deteriorate BFO photocatalytic activities when they are used as photocatalysts. For instance, Ke et al. [14] have reported that secondary phases are presented during the synthesis of BFO via a co-precipitation method though the processing factors are carefully controlled.

As we know, as a dispersant, PVA has the reticular structure. In the present investigation, a PVA-assisted solid state reaction processing was used to prepare BFO particles. The formation of large size particles could be effectively confined due to the presence of

*To whom correspondence should be addressed: Email:yuexiang65@hotmail.com
Phone: +86-571-86875612, Fax: +86-571-86875694

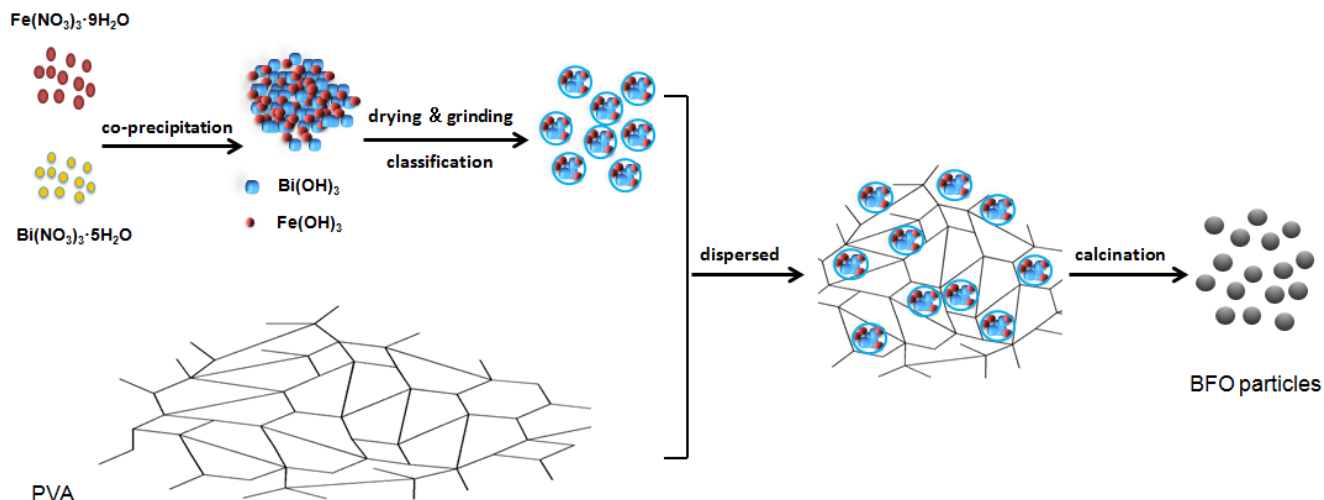


Figure 1. Schematic diagram for preparation of BFO particles

the reticular structure of PVA during the synthesis process. In such a process, BFO xerogel precursor was prepared by a co-precipitation process. After pulverization and classification, the BFO xerogel precursor particles were dispersed in a PVA solution. Finally the mixture of BFO precursor particles and PVA were heat treated at a given temperature to synthesize BFO particles. The addition of PVA and classification of BFO precursor particles are expected to prevent particle agglomeration during the heat treatment process and to control the particle size respectively. The characteristics of the as-prepared BFO particles are reported and its photocatalytic activity was also evaluated by photodegradation of methyl orange (MO) under visible-light irradiation.

2. EXPERIMENTAL

2.1. Synthesis of Catalyst

The starting materials used in the present work included analytical grade ferric nitrate, bismuth nitrate, potassium hydroxide and polyvinyl alcohol.

As the schematic diagram shown in Fig. 1, BFO particles were synthesized through a PVA-assisted solid state reaction processing. In a typical synthesis procedure, bismuth hydroxide and ferric hydroxide are co-precipitated by potassium hydroxide from a ferric nitrate and bismuth nitrate solution. After drying, the BFO xerogel precursor including $\text{Fe}(\text{OH})_3$ and $\text{Bi}(\text{OH})_3$ was ground into fine powders through a mortar and pestle and then sieved by a standard sieve (120 mesh). 1.5 g fine xerogel powder was put into a PVA aqueous solution (250 ml distilled water with 5 g PVA). After keeping stirring and evaporation for 8 h under a temperature of 80 °C, a brown viscous liquid was obtained. Then the brown viscous liquid was spread onto a glass to form a piece of sheet. After being cut into pieces, the sheet was heat treated in a muffle furnace according to a given heating schedule. For comparison, BFO particles were also synthesized by directly heat treated in a muffle furnace using the obtained BFO xerogel precursor as the initial materials.

2.2. Characterizations

Thermo-gravimetry (TG) and differential scanning calorimetry (DSC) were carried out in a temperature ranges of 30-800 °C with a heating rate of 10 °C·min⁻¹ on a Mettler Toledo SMP/PF7458/MET/600W instrument to investigate the thermal reaction of BFO xerogel precursor which guided the synthesis of pure BFO particles. The phase structure of the powder was identified by a Bruker D2 X-ray diffractometer (XRD) using CuK_α radiation and the morphology was observed using a high resolution transmission electron microscope (HRTEM, JEOL JEM-2100). Optical absorption spectrum was recorded on a Shimadzu UV-3600 UV-visible spectrophotometer.

2.3. Photocatalytic Test

The photocatalytic behavior of the as-synthesized BFO nanoparticles (0.2 g) was evaluated by photodegradation of methyl orange (MO, $\text{C}_{14}\text{H}_{14}\text{N}_3\text{O}_3\text{SNa}$) in aqueous solution (5 mg/L) under visible-light irradiation using a 300 W Xe lamp with a cutoff filter ($\lambda \geq 420$ nm) under a neutral pH condition. In order to prevent any self-degradation of MO, the degradation of MO without any BFO powders in the same condition was added.

3. RESULTS AND DISCUSSION

3.1. Thermal Analysis

Fig. 2 (a) shows the TG-DSC curves of the obtained xerogel sheet containing PVA at a heating rate of 10 °C·min⁻¹. A sharp exothermic peak can be observed at around 400 °C on the DSC curve and the corresponding TG curve can be roughly classified into three steps. The first weight loss of about 9 wt.% can be ascribed to the removal of adsorbed water in the xerogel. The second weight loss step of about 16 wt.%, associated with two small endothermic peaks located at 228 and 255 °C in the DSC curve shown in Fig. 2 (b), might be due to the dehydration of $\text{Bi}(\text{OH})_3$ and $\text{Fe}(\text{OH})_3$. The observed 16 wt% weight loss is close to the calculated weight loss value of 14.7 wt% according to the precursor com-

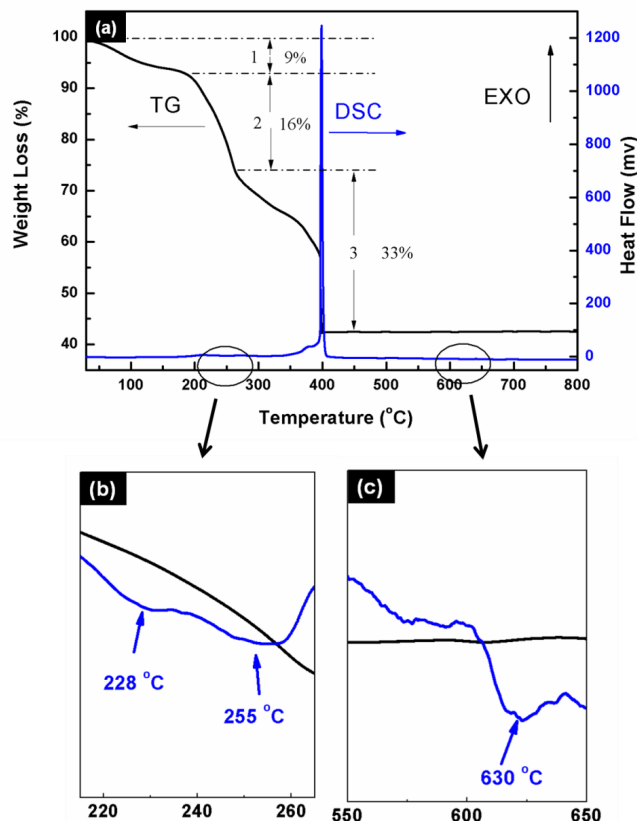


Figure 2. (a) TG-DSC curves of the PVA-assisted BFO precursor xerogel, (b) and (c) the details of TG-DSC curves in the specified temperature ranges

position, further confirming the dehydration of Bi(OH)₃ and Fe(OH)₃ taking place during this period. The third weight loss process with a pronounced exothermic peak is obviously due to the oxidation of PVA. A small endothermic peak is observed at 630 °C as shown in Fig. 2 (c) which corresponds to the crystallization of BFO powders. This process would not yield weight loss as identified by the corresponding TG curve.

3.2. Phase Structure

The XRD patterns of the sample after heat treated are shown in Fig. 3. All diffraction peaks can be indexed as a rhombohedral phase with the space group R3m (JCPDS no. 72-2112). No other crystalline phase is detected, indicating that pure crystalline BFO phase can be obtained by the present PVA-assisted solid state reaction processing method, while the second phase Bi₂₅FeO₄₀ appears for BFO powder prepared without grinding, sieving or PVA optimized processing. The result means that the homogeneity of Bi(OH)₃ and Fe(OH)₃ constituents with addition of PVA which are obtained in the co-precipitation process can be maintained during the following grinding, sieving and heat treatment to produce pure crystalline BFO phase.

3.3. Microstructure Analysis

The TEM photographs of the obtained BFO powder with an

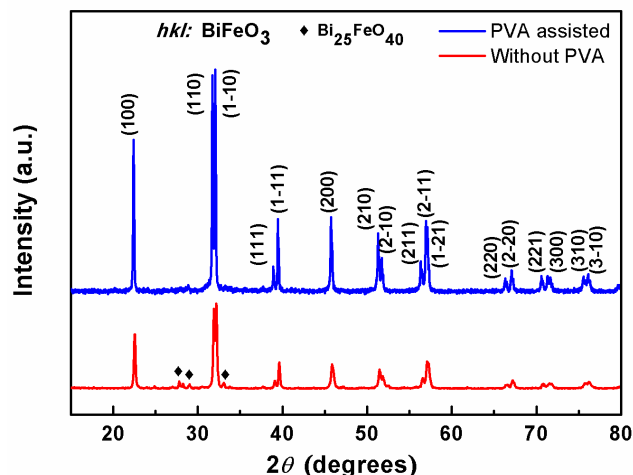


Figure 3. XRD patterns of the as-synthesized BFO powder with and without addition of PVA

irregular morphology are shown in Fig. 4. As can be clearly seen from Fig. 4 (a), the as-prepared BFO particles are well-dispersed and the agglomerate size is from 100 to 200 nm which has the better dispersity than that of BFO produced without addition of PVA shown in Fig. 4 (b). From the HRTEM photograph shown in Fig. 4(c), it is clearly demonstrated that the BFO agglomerate is composed of grains with different orientations and that grain sizes are in a range from 5 to 10 nm. In the typical grain crystals, the measured crystal interplanar spacing are 0.392 nm and 0.279 nm toward Fig. 4 (a). Coupling with the XRD result shown in Fig. 3, the crystal planes in Fig. 4 (c) can be determined as (100) and (110) planes, and the crystal planes in Fig. 4 (d) can be determined as (200) and (110) planes.

3.4. Proposed Mechanism of the Formation of BiFeO₃

Based on the above observations, the BFO particle formation in the present PVA-assisted solid state reaction process is tentatively proposed. During the co-precipitation process, the BFO precursor xerogel containing Bi(OH)₃ and Fe(OH)₃ in a stoichiometric ratio is obtained. After grinding and sieving, it is obvious that the selected precursor xerogel is homogeneous. The addition of PVA with a reticular structure can further make the xerogel uniform and confine the sintering and unlimited growth of BFO particles during the calcination process. This leads to the formation of pure nanosized BFO particles with well dispersity as diagrammatically demonstrated in Fig. 1.

3.5. Optical absorption property

As shown in Fig. 5, the diffuse reflection spectrum have been transformed into the absorption one according to the Kubelka-Munk theory. The calculated band gap from the plot of the Kubelka-Munk function [15] is ~2.1 eV, as presented in Fig. 5 inset. This indicates that the as-prepared BFO material has the potential visible light response for photocatalytic degradation.

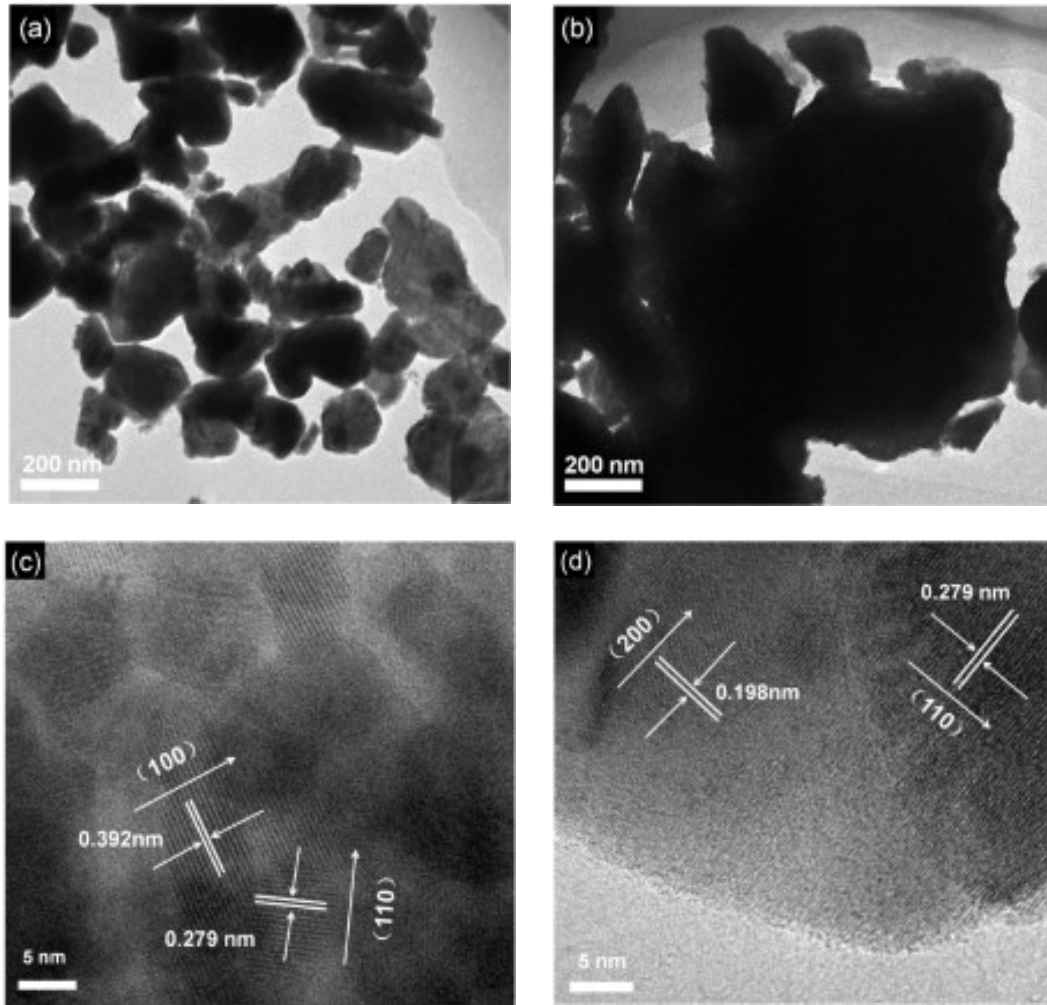


Figure 4. (a) TEM photograph of the as-synthesized BFO particles with addition of PVA; (b) TEM photograph of the as-synthesized BFO particles without addition of PVA; (c) and (d) HRTEM of BFO crystal lattice structure from (a) and (b) respectively

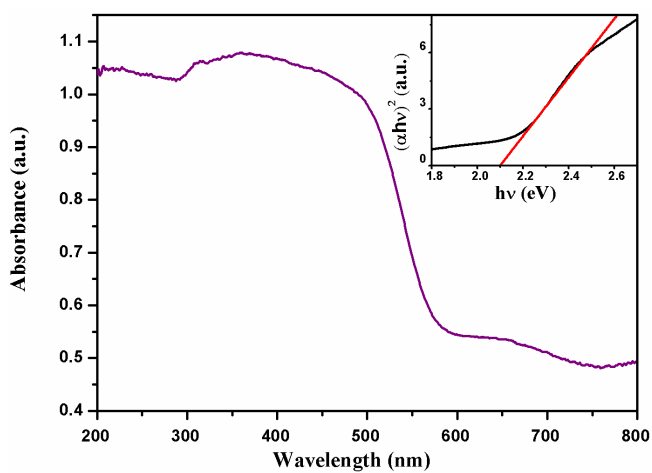


Figure 5. UV-vis absorption spectra of the BFO particles synthesized with addition of PVA. Inset is the plot of the band gap energy

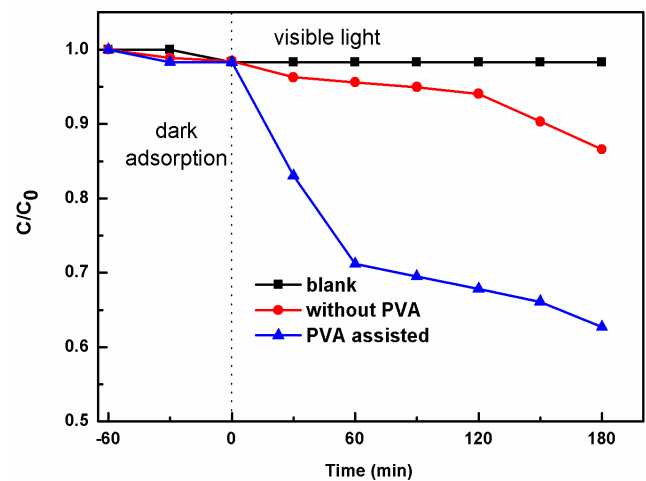


Figure 6. Photocatalytic degradation of MO as a function of the irradiation time under visible-light using BFO powders synthesized with and without addition of PVA

3.6. Photodegradation Activity

It was considered that the particle morphology, size, phase purity, dispersity and crystallinity of a photocatalyst would significantly influence its photocatalytic activity [5]. Fig. 6 shows the photodegradation of MO as a function of the irradiation time under visible-light by the as-prepared BFO nanoparticles. After 3 h irradiation, about 38 % of the MO was photolyzed using BFO powder synthesized with addition of PVA. While the degradation rate of BFO prepared without addition of PVA is only 15 %. The result demonstrates that the BFO material with nanoscale and well dispersity synthesized through the present PVA-assisted solid state reaction process possesses obvious photocatalytic activity under visible-light irradiation, suggesting that it is a promising candidate as a visible-light response photocatalyst.

4. CONCLUSIONS

In summary, pure BFO particles were synthesized by a PVA-assisted solid state reaction process through dispersing the classified BFO precursor xerogel particles into PVA solution prior to heat treatment. The obtained BFO agglomerates exhibit pure polycrystalline phase with well dispersity in nanoscale. The agglomerate is composed of various small crystal grains with different orientations. The obtained BFO nanoparticles exhibit more efficient photocatalytic activity under visible-light irradiation than that of BFO particles synthesized without addition of PVA, which further proves that BFO material with well dispersity in nanoscale has higher photocatalytic activity.

5. ACKNOWLEDGEMENTS

This work is financially supported by the National Natural Science Foundation of China (No. 51372237), International S&T Cooperation Program of China (No. 2013DFG52490), Public Welfare Project of Science & Technology Department of Zhejiang Province (No. 2014C31026) and Zhejiang Provincial Higher School Talent Project (No. PD2013183).

REFERENCES

- [1] G Catalan, J. F. Scott, *Adv. Mater.*, 21, 2463 (2009).
- [2] F Gao, X. Y. Chen, K. B. Yin, S Dong, Z. F. Ren, F Yuan, T Yu, Z. G. Zou, J. M. Liu, *Adv. Mater.*, 19, 2889 (2007).
- [3] C. Karunakaran, S. SakthiRaadha, P. Gomathisankar, *Mater. Express*, 2, 319 (2012).
- [4] T Gao, Z Chen, Y. X. Zhu, F Niu, Q. L. Huang, L. S. Qin, X. G. Sun, Y. X. Huang, *Mater. Res. Bull.*, 59, 6 (2014).
- [5] W. M. Tong, L. P. Li, W. B. Hu, T. J. Yan, G. S. Li, *J. Phys. Chem. C*, 114, 1512 (2010).
- [6] M. Yasin Shamia, M. S. Awan, M Anis-ur-Rehman, *J. Alloy. Compd.*, 509, 10139 (2011).
- [7] Y. Q. Zheng, G. Q. Tang, H. Y. Miao, A Xia, H. J. Ren, *Mater. Lett.*, 65, 1137 (2011).
- [8] N. Das, R. Majumdar, A. Sen, H. S. Maiti, *Mater. Lett.*, 61, 2100 (2007).
- [9] X. L. Chen, Y Tang, L Fang, H Zhang, C. Z. Hu, H. F. Zhou, *J. Mater. Sci: Mater. Electron.*, 23, 1500 (2012).
- [10] G. Q. Tan, Y. Q. Zheng, H. Y. Miao, A Xia, H. J. Ren, *J. Am. Ceram. Soc.*, 95, 280 (2012).
- [11] C Reitz, C Suchomski, C Weidmann, T Brezesinski, *Nano Res.*, 4, 414 (2011).
- [12] C. J. Tsai, C. Y. Yang, Y. C. Liao, Y. L. Chueh, *J. Mater. Chem.*, 22, 17432 (2012).
- [13] A. Chaudhuri, S. Mitra, M. Mandal, K. Mandal, *J. Alloy. Compd.*, 491, 703 (2010).
- [14] H Ke, W Wang, Y. B. Wang, J. H. Xu, D. C. Jia, Z Lu, Y Zhou, *J. Alloy. Compd.*, 509, 2192 (2011).
- [15] P. Kubelka, F. Munk, *Tech. Z. Phys.*, 12, 593 (1931).